He-diamond interaction probed by atom beam scattering

G. Vidali* and D. R. Frankl
Department of Physics, The Pennsylvania State University, University Park, Pennsylvania 16802
(Received 19 August 1982)

A ^{4}He atomic beam was used to probe the He-C (diamond) interaction. Selective adsorption features have been measured and three energy levels identified: 6.4, 3.0, and 1.1 meV with a standard deviation of 0.1 meV. Diffraction patterns showed weak diffraction up to the second order; a corrugation parameter of 0.021 Å was obtained with the use of a hard-wall model in the eikonal approximation. An extensive study of surface preparation was carried out and the results of ^{4}He diffraction for different methods of surface cleaning are reported.

I. INTRODUCTION

Scattering of atomic beams at thermal energies is now recognized as an important tool in surface science, capable of yielding information on crystallographic structure,[1-4] interaction potentials,[5,6] and phonon dispersion.[7] Helium scattering from the basal plane of graphite has been extensively studied in this laboratory[5] and at the University of Genoa.[6] Selective adsorption energies and matrix elements of the Fourier components of the periodic part of the interaction potential were used to generate a good description of the potential and to calculate the two-dimensional band structure of a He atom on the graphite basal plane.[8] These band-structure calculations gave binding energies and low-coverage specific heats in very good agreement with those from thermodynamic measurements.[9]

Here we report the study of the He-C (diamond) interaction through the scattering of ^{4}He atoms from the (111) surface of diamond. The main goal of this study was to compare the interaction of He with the two forms of carbon. Previous attempts at atom scattering from diamond[10] had given only diffuse, structureless distributions. However, some recent electron experiments have produced extremely interesting results. For example, low-energy electron diffraction (LEED) studies[11,12] showed that low-index diamond surfaces can reconstruct to $(2\times2)/(2\times1)$ (a 2×2 surface cannot be distinguished by LEED from a three-domain 2×1 structure) although the exact conditions under which this happened were not clear. Photoemission[13] and electron energy-loss spectroscopy[14] studies suggested that there are no electronic surface states on the unreconstructed (111) surface. This result was unexpected since theoretical calculations[15] and comparison with other semiconductor surfaces[16] suggested the opposite. It has been proposed[17] that the lack of surface states is due to chemisorption of hydrogen on the surface. This hypothesis was reinforced by the observation[14,18] of surface states accompanying the reconstruction to $(2\times2)/(2\times1)$ after annealing at $T>900$ °C. This suggested that the H atoms desorbed at $T\simeq900$ °C.

We studied this transition both by atom beam diffraction and LEED. In addition, we identify three selective adsorption levels on the unreconstructed surface, and obtain some preliminary estimates regarding the interaction potential.

II. EXPERIMENTAL METHODS

A. Apparatus

As the apparatus has been described previously,[19] only a brief outline is given here. A supersonic ^{4}He beam ($\Delta\lambda/\lambda\simeq2\%$ for the 17.3-meV beam) is produced by expanding high-pressure He gas ($\simeq35$ atm) through a 7-μm nozzle. Beam energies of 63.2 meV (room temperature) and 17.3 meV (liquid-nitrogen temperature) were used. The collimated beam ($\Delta\theta<10^{-3}$) is chopped for in-phase detection and then enters an UHV chamber where it impinges on the surface. The main chamber is evacuated by a cryopump in a closed-cycle refrigerator. After a 2-day bake at $T\simeq160$ °C the pressure is in the middle 10^{-11} Torr (base pressure) or low 10^{-10} Torr (working pressure). The outgoing beams are detected by a movable quadrupole mass spectrometer with an acceptance angle of $\simeq1°$. Typical relative intensities of 5×10^{-4} can be measured with a lock-in detector with a time constant of $\simeq1$ sec. A LEED-Auger optics is included in the scattering chamber.

The sample studied is a natural single diamond crystal ("macle," Ref. 20) of triangular shape with a 5-mm side and 2.5-mm thickness; the two parallel faces are the (111) faces. It is mounted with three

small tabs on a tantalum plate. The plate can be heated up to 1300 °C by electron bombardment from the back. Great care has been taken in cleaning the tantalum plate to avoid contaminating the sample during heating. The plate was etched with a solution of H_2SO_4, HNO_3, and HF and then thoroughly rinsed with solvents. Furthermore, all sources of electrons (ion gauge, heater, detector ionizer) have been put out of sight of the sample since there are reports[14] that electron bombardment can cause structural modifications.

B. Surface preparation

Owing to the extreme sensitivity of atom scattering to surface conditions, considerable effort was required to obtain a suitable surface. More details on surface preparation methods are given in Ref. 21. Some of the more common methods of surface preparation were inapplicable. For example, *in situ* cleavage was not possible for our small crystal, and ion bombardment is known to cause extensive damage[12] that cannot be annealed out. Various methods of cleaning the surface were tried and the results were assessed by atom reflection and diffraction and sometimes by LEED. On some occasions it was possible to obtain reasonably clear LEED patterns but no specular He reflection. A summary of the methods and results is given in Table I. The early attempts at mechanical polishing were made with micrometer-size diamond paste on a soft cloth lap at low speed.[12] The first of these was quite successful giving about 5% specular reflection. However, an attempt to improve this by annealing *in vacuo* at $T \simeq 1000$ °C destroyed the surface. Attempts to restore it by heating (up to 1300 °C) with and without H_2 ($p \simeq 10^{-6}$ Torr) or O_2 ($p \simeq 10^{-8}$ Torr, $T \simeq 800$ °C) failed. The idea behind this treatment was chemically to remove any disordered carbon or impurity atoms from the surface.

We next tried light mechanical polishing followed by chemical etching with various mixtures of concentrated acids (H_2SO_4, $HClO_4$, HNO_3) according to empirical recipes found in the literature.[22] Surfaces prepared in this way gave weak specular reflection after annealing at temperatures of the order of 800 °C. The specular peaks were typically 1% or less of the incident beam and broader than expected, indicating either a highly disordered or contaminated surface. Consequently, we returned to the mild polishing described above but with little improvement. Finally, we went to a much more vigorous polishing on a cast-iron wheel at about 700 ft/min under a few pounds loading. The final surface looked very smooth and mirrorlike with complete removal of markings that had persisted throughout the previous treatments. The sample was, as always, thoroughly rinsed with water and then with solvents before being mounted on the sample holder. This type of polishing gave the best results to date in terms of intensity, stability, and reproducibility.

Most of the data described below were taken after the first such polishing. Then there followed a series of heat treatments that led to an irreversible

TABLE I. Comparison of surface preparation methods. This table summarizes the various methods that were tried to prepare the surface and the results in terms of helium reflection. Method 1: light mechanical polishing. Method 2: light mechanical polishing followed by acid treatment. Method 3: vigorous mechanical polishing (details in the text). Atomic hydrogen is produced using the filament of an ion gauge, see Ref. 14. For the surface annealed at $T \approx 990$ °C (method 3) a LEED pattern showed reconstruction.

Method	Heat treatment *in vacuo*	Results
1	after bake	good signal
	annealing $T \lesssim 900$ °C	better signal
	annealing $T \gtrsim 900$ °C	worse signal
	annealing + H_2, O_2	no signal
2	after bake	no signal
	annealing $T \lesssim 900$ °C	little signal
3	after bake	good signal
	annealing $T \lesssim 900$ °C	best signal
	annealing + H ($p \simeq 10^{-5}$ Torr, $\simeq 10$ min)	no change
	annealing $T \approx 950$ °C	little signal, reconstruction
	annealing $T \approx 990$ °C	no signal
	annealing + H ($p \simeq 10^{-5}$ Torr, $\simeq 10$ min)	no change

change to a much less reflective surface. A second polishing failed to give comparable results, possibly because there was an interval of several weeks of exposure to room air before insertion into the vacuum. For both of these polishings, the sample had been mounted with a hard wax (C-70), and we conjectured that some traces of this might have remained. Treatment with a strong oxidizing acid mixture (potassium dichromate in hot concentrated perchloric acid) failed to restore the surface. We carried out the third polishing in a specially constructed mechanical clamp. This was successful and gave results comparable with the first.

C. Selective adsorption measurements

Part of this study consisted of the determination of the bound-state energy levels of the ^{4}He-C (diamond) potential. As shown later, the determination of these energies involves accurate measurements of the initial and final kinematic conditions. The incident wave-vector magnitude $|k|$ can be measured at 0.5% accuracy using a mechanical velocity selector. The incident polar angle θ_s and the detector angle θ_d in the plane of incidence are controlled by stepping motors and read to 0.1°. The azimuthal angle ϕ is read on a vernier mounted directly on the sample holder with an accuracy of 0.2°. All these errors combined would amount to an uncertainty in the energy levels of 0.13 meV (conservative estimate). Other systematic errors may be introduced by various misalignments. Prior to the insertion of the sample into the apparatus the beam is accurately positioned to pass through the axis of polar rotation of the sample holder. The crystal is mounted so that the surface is, as nearly as possible, tangent to this axis. However, some misalignments still remain due to uncertainties in positioning, surface faceting, etc. There errors can be accounted for by doing a "calibration run," in which the angular position of the specular beam is measured for many incident angles. Ideally, a plot of θ_d vs θ_s would give a straight line with a slope of -2.00. In reality, one obtains a set of points that lie more or less on a straight line with a correlation coefficient of typically -1.0×10^{-5} and a slope of -2.05. A calculation of θ_d vs θ_s that takes into account the misalignments mentioned above was performed and it was found that in most cases the linear approximation is adequate. All the angles reported below have been corrected in this way.

III. RESULTS

The results presented here are for the surface mechanically polished as discussed above unless specified. After the surface was inserted into the apparatus and the system was baked at 160 °C for 2 or 3 days, a He specular reflection of typically 5% of the incident beam was obtained. It dwindled down to 2–3 % after 3–4 days. Annealing at $T\simeq800$ °C but lower than 900 °C brought the specular beam intensity up to 8%, and resonance and diffracted features became more pronounced. Two sets of measurements were taken. In the first the detector was scanned for a given incident angle θ_s and the diffracted beams were recorded. In Fig. 1 the reciprocal lattice for the (111) diamond surface is sketched and the convention to label the two-dimensional reciprocal-lattice vectors $\vec{G}=(l,m)$ is shown. The lattice parameter for the (111) surface is 2.52 Å. Typical actual traces of diffraction patterns for $E_i=63.2$ meV are shown in Figs. 2 and 3 along the two principal azimuths. Diffracted beams up to the second order, i.e., for $\phi=30°$ according to Fig. 1, were detected. Diffracted beams were measured for various angles of incidence. Their intensities were always much smaller than the specular peaks at the same incident angle. Comparable results were obtained with $E_i=17.3$ meV except that the angular width of the diffracted beams was smaller due to the narrower incident velocity distribution. The angular position of the diffracted beams is in agreement with the bulk lattice.

In a separate set of measurements for selective adsorption the specular intensity was monitored as a function of the incident angle. Sharp features are detected in such a plot when a He atom goes into a selective adsorption state, or "bound-state resonance." The actual measurement is done by sweeping the detector continuously and stepping the surface typically by 1/4° so that the specular maximum is recorded repetitively. The procedure is repeated

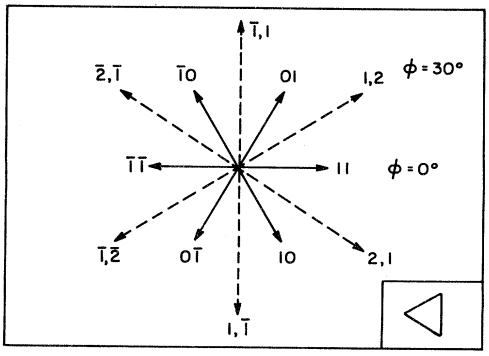

FIG. 1. Reciprocal lattice for the diamond (111) surface with convention for labeling $\vec{G}=(l,m)$. Dashed lines represent second-order reciprocal-lattice vectors. In the inset the orientation of the "macle" is shown.

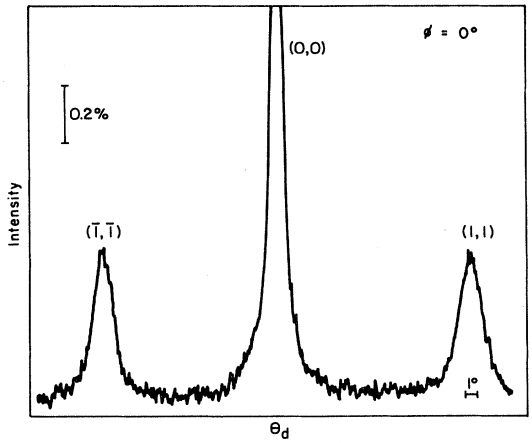

FIG. 2. Actual trace of detected intensity vs detector angle. The intensity is given as percentages of the incident beam. The ratio of the specular to diffracted intensity is approximately 5. $E_i=63.2$ meV, $\theta_s=23.5°$, $\phi=0°$.

for different azimuthal angles ϕ. Typical plots are presented in Figs. 4 and 5. In Fig. 4 a comprehensive polar scan of specular intensity is shown. The labeled features are attributed to bound-state resonances and are reproducible for different days and surfaces. Since this scan is taken slightly off the crystallographic symmetry direction, the two different $\vec{G}=(l,m)$ vectors for each energy level are separated. In Fig. 5 similar scans are presented for different values of the angle ϕ; such scans help in assigning the energy levels and can show splittings as explained in the discussion. In total, over 80 resonances were observed and assigned to three energy levels. The data were taken with an $E=17.3$ meV beam. No features could be detected using the higher-energy beam, probably due to the increased

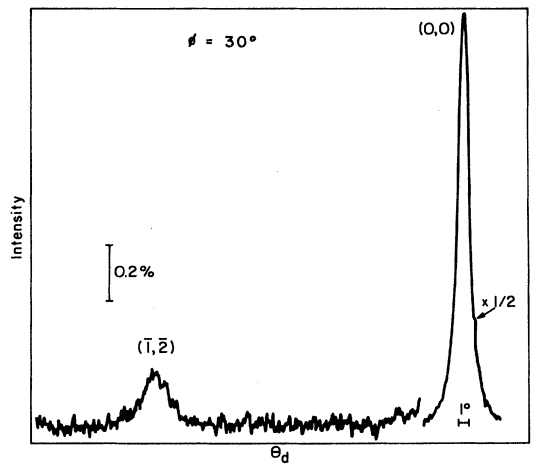

FIG. 3. Same as in Fig. 2 but for $\phi=30°$.

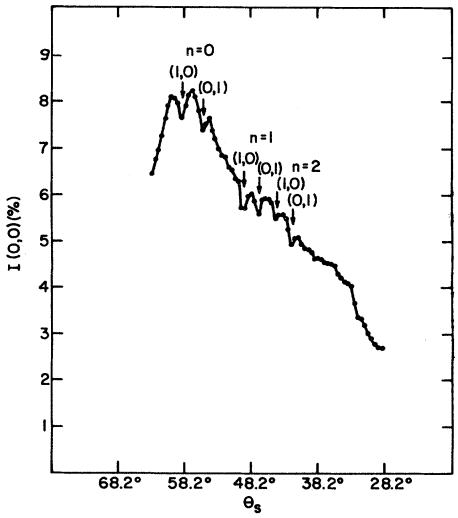

FIG. 4. Specular intensity, in percent of the incident beam, vs incident angle θ_s. Labeled arrows show resonances of order n and reciprocal-lattice vector $\vec{G}=(l,m)$. $E_i=17.3$ meV and $\phi=2.5°$.

incident velocity spreading that broadens the already weak features.

IV. DISCUSSION

A. Bound-state resonances

An incoming atom has to satisfy the kinematic conditions which, for free-particle motion parallel to

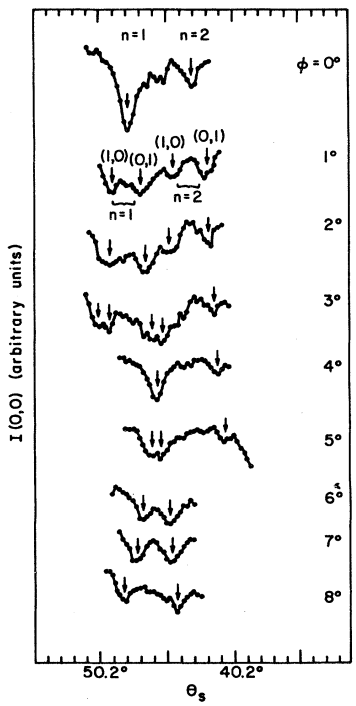

FIG. 5. Same as in Fig. 4 but for different ϕ's.

the surface, read

$$\vec{K}_i+\vec{G}_{l,m}=\vec{K}_f\ , \tag{1}$$

$$(\vec{K}_f)^2+k_{fz}^2=k_i^2\ , \tag{2}$$

where $\vec{k}$ is the incident wave vector and $\vec{K}$ is its projection parallel to the surface. The conservation of parallel momentum, Eq. (1), and energy, Eq. (2), can be combined to give

$$(\vec{K}_i+\vec{G})^2+k_{fz}^2=k^2\ . \tag{3}$$

Resonance occurs when $k_{fz}^2=-2m\mid E_n\mid/\hbar^2$, where E_n (<0) is the energy of the nth bound state $(n=0,1,\ldots)$. Then Eq. (3) describes in a K_x-K_y plane the equation of a circle with radius

$$R=\left[k^2+\frac{2m}{\hbar^2}\mid E_n\mid\right]^{1/2}$$

centered at $-\vec{G}_{l,m}$.

From the measurement of θ_s, ϕ, and $\mid k\mid$, the position of a resonance can be plotted in K_x-K_y space and the values of E_n can be readily obtained. All the resonances (except those for $\phi=30°$) have been reported in Fig. 6; different symbols are used for data obtained on different days. The values of the energy levels and their standard deviations are reported in Table II; for comparison, the energy values for ^{4}He-graphite[5] are also given. A Lennard-Jones (LJ) 3-9 potential of the form[23]

$$V(z)=3^{3/2}\frac{D}{2}\left[\left[\frac{\sigma}{z}\right]^9-\left[\frac{\sigma}{z}\right]^3\right] \tag{4}$$

was fitted to the three levels reported in Table II. Since at large distances the potential becomes[24]

$$V(z)\sim -C/z^3\ , \tag{5}$$

from Eq. (4) we obtain $C_3=3^{3/2}\sigma^3 D/2$. C_3 has been recently calculated to be 204 meV Å^3 (Ref. 25); therefore, the well depth D can be chosen to be the only free parameter. The value of D so determined, 9.39 meV, can be compared to that for He-graphite, i.e., $\simeq$14—15 meV, depending on the potential chosen. It is interesting to note that the He-graphite data, with the use of eight measured energy levels (for ^{3}He and ^{4}He), could not be fitted to a Lennard-Jones 3-9 potential using the correct C_3 value.[26] Three comments should be made. The first is that a deep-lying energy level for He-diamond seems to be missing. A careful search for this level gave no result. The second comment is that the depths of the selective adsorption features (10% of the specular beam) are much shallower for He-diamond than for He-graphite. Finally, contrary to the He-graphite case, no splitting of degenerate resonances could be resolved. A splitting occurs [Eq. (5)] when $\vec{K}$-plane circles described by Eq. (3) cross each other. In this neighborhood of $\vec{K}$ space the two-dimensional free-particle approximation breaks down and Eq. (3) is not valid. The Fourier components $V_{\vec{G}}(z)$ of the potential

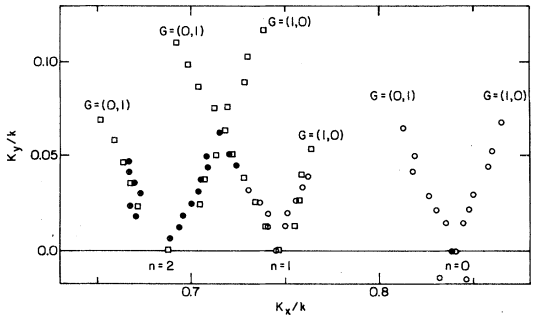

FIG. 6. Resonances plotted in K_x-K_y space. Different symbols are for runs on different days.

$$V(\vec{r})=V_0(z)+\sum_{\vec{G}\neq 0}V_{\vec{G}}(z)\exp(i\vec{G}\cdot\vec{R})$$

lift the degeneracy, and matrix elements $\langle j\mid V_{\vec{G}}\mid j'\rangle$ connecting the degenerate states can be measured. Most of the resonances were associated with either $\vec{G}=(0,1)$ or (1,0); the Fourier component of the potential connecting these resonances is $V_{\vec{G}}=\bar{1},1$ and is second order. A good candidate for such a splitting is the crossing of $E_{n=1}$, $\vec{G}=(0,1)$ with $E_{n=2}$, $\vec{G}=(1,0)$ levels. As seen from

TABLE II. Experimental and calculated energies for ^{4}He-diamond. Experimental energies for ^{4}He-graphite from Ref. 6 are also shown. All values in meV.

	^{4}He-diamond		^{4}He-graphite
n	$\mid\epsilon_n\mid$ (Expt.)	$\mid\epsilon_n\mid$ (LJ 3-9)	$\mid\epsilon_n\mid$ (Expt.)
0	−6.44±0.13	−6.49	−12.06±0.12
1	−3.01	−2.88	−6.36
2	−1.10	−1.13	−2.85
3		−0.37	−1.01
4		−0.09	−0.17

Fig. 5 there is no resolvable splitting at the crossing ($\phi=4°$, $K_y\cong 0.06k$); a more careful investigation (scans taken every 0.2° in ϕ) confirmed this result.

Resonances associated with $\vec{G}=(1,1)$ were very weak and detectable only near $\phi=0°$; therefore, no crossing with $\vec{G}=(0,1)$ could be detected (it would have involved a first-order Fourier component of the potential). The comments made above are consistent with the hypothesis that the He-diamond interaction potential is weaker and smoother than the He-graphite one. Further evidence for this is given below.

B. Diffraction

First- and second-order diffracted intensities were typically $<20\%$ of the specular intensity at the same incident angle both with the 17.3- and 63.2-meV incident beams. The diffraction pattern was analyzed with the corrugated hard-wall model with a well in front.[27] The main reason for using such a model is to compare the results of this study to the He-graphite system that has been analyzed in the same way.[6] In a hard-wall model[27] the surface is described by a corrugation function

$$\xi(\vec{R})=\sum_{\vec{G}\neq 0}\xi_{\vec{G}}\exp(i\vec{G}\cdot\vec{R})\ .$$

The wave function vanishes at the surface and inside. An attractive well is introduced in front of the wall to take into account the increased perpendicular momentum of the particle near the classical turning point. Thermal effects are neglected. If only the first Fourier component ξ_{10} in Eq. (5) is used, we have

$$\xi(x,y)=2\xi_{10}\left[\cos\frac{2\pi x}{L}+\cos\frac{2\pi y}{L}+\cos\frac{2\pi}{L}(x+y)\right],$$

where here x and y are along the lattice vectors and L is the lattice parameter. The scattering problem is solved in the eikonal approximation[27] where, essentially, multiple scattering is neglected; this should be a good assumption in this case, where diffracted intensities are much smaller than specular ones. The probability of a particle being diffracted via a reciprocal-lattice vector $\vec{G}$ is[27]

$$P_{\vec{G}}=\frac{|k_{iz}|}{|k_{fz}|}\left|\frac{1}{A}\int\exp\{-i[\vec{G}\cdot\vec{R}+q\xi(\vec{R})]\}d^2R\right|^2,$$

where the integral is over the unit cell of area A. The momentum transfer is

$$q=k_i\left[\left[\cos^2\theta_i+\frac{D}{E_i}\right]^{1/2}+\left[\cos^2\theta_{\vec{G}}+\frac{D}{E_i}\right]^{1/2}\right],$$

where $\theta_{\vec{G}}$ is the final scattering angle, $D=9.4$ meV is the well depth (see Sec. IV A), and $E=17.3$ meV is the incident energy.

The data used in the analysis were obtained at both energies. In Fig. 7 experimental and theoretical probabilities for several diffracted beams are reported. The theoretical probabilities have been reduced by a common factor (≈ 10) to be compared with the experimental ones. This factor indicates the amount of inelastic or diffuse scattering. From a fit of the data a corrugation parameter $\xi_{10}=0.021\pm 0.002$ Å is obtained.[28] This is comparable with $\xi_{10}=0.023\pm 0.002$ Å for He-graphite.[6] The maximum corrugation amplitude for He-graphite is 0.21 Å and is small compared to He-LiF(001), 0.61 Å,[29] or He—Cl—$c(2\times 2)$-Ag(100)$\simeq$1 Å,[4] but 10 times larger than for He-Ag(111).[30] The main uncertainties in this procedure lie in the subtraction of inelastic or incoherent events; this subtracted part may be a good fraction of the recorded signal, since the diffracted features are very weak.

Laughlin[31] has calculated the He-diamond potential with the use of a semiempirical method.[32] The diamond charge density is taken to be the sum of carbon-atom charge densities, and a known value of the van der Waals coefficient C_3 (Ref. 25) was used. The result, a very smooth and shallow potential with a turning point at 2.9 Å, considerably higher than for He-graphite,[8] is consistent with the evidence presented above. However, his well depth, $\approx$4 meV, seems too shallow; the same discrepancy is found

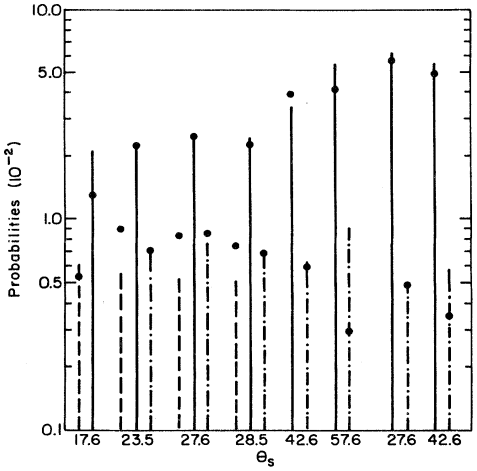

FIG. 7. Comparison of experimental (filled circles) with theoretical (bars) probabilities for several specular (solid lines) and diffracted beams [for $\vec{G}=(1,1)$, dashed line; for $\vec{G}=(\bar{1},\bar{1})$, dashed-dotted line]. The numbers at the bottom of the figure give the incident angles. The incident energy is 63.5 meV except for the beams at the far right ($\theta_s=27.6°$, 42.6°; $E_i=17.3$ meV).

also in his potential for He-GeAs(110) (Ref. 32), where the experimental well depth is reproduced but the C_3 coefficient he derives is twice the calculated one.[25] The attractive part of the potential, determined by the coefficient C_3, Eq. (5), is comparable for He-diamond and He-graphite[25,26]; however, the turning point for He-diamond is projected further out and therefore it is plausible that the total potential experienced by the atom has a shallower well depth for diamond than for graphite.

V. RECONSTRUCTION

As mentioned earlier it has been observed that a reconstruction takes place on annealing at $T \gtrsim 900$ °C.[14,18] Two experiments were done to study this transition; in both cases the surfaces used were considered to be "good" surfaces before the treatment. In the first experiment the sample was annealed in steps of increasing temperatures from 800 °C for 5 min each. Since the temperature is measured with an optical pyrometer, the values are only indicative, but do agree with other works.[14,18] The specular intensity was followed by a cool-down period of 15 min after each annealing cycle (cycles at 815, 855, 875, 910, and 955 °C). After the last cycle the signal dropped to less than one-third of the untreated sample (this cannot be attributed to a Debye-Waller factor, as will be discussed below). A LEED pattern taken after this annealing showed a $(2\times2)/(2\times1)$ reconstruction. A careful study of the He-diffraction pattern showed that in addition to the first-order peak there was also a half-order

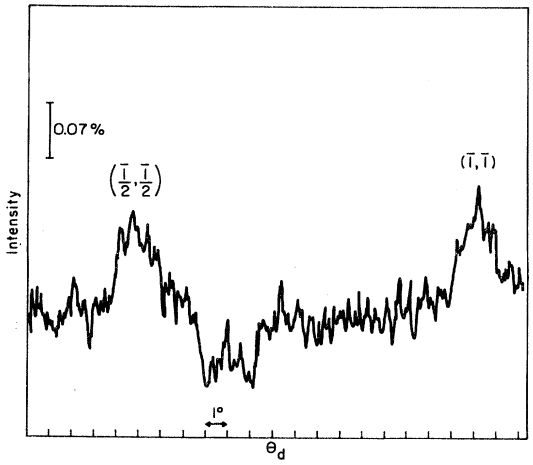

FIG. 8. Diffraction peaks for the reconstructed surface. The specular peak is ~1% of the incident beam. $\theta_s = 38.5°$, $E_i = 17.3$ meV.

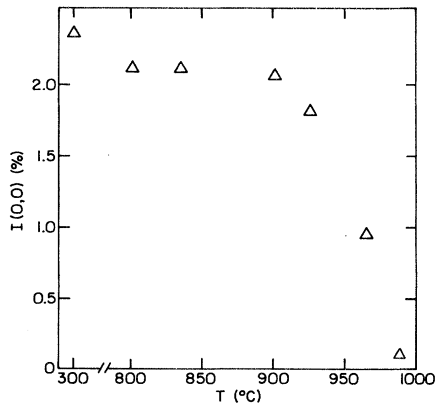

FIG. 9. Specular intensity $I(0,0)$ vs T (°C).

one, as shown in Fig. 8. These features were reproduced on other days. In the second experiment a good surface was annealed as before at temperatures of 800, 835, 900, 925, 965, and 990 °C. In this case the heating cycles were consecutive without cool-down periods and the specular beam was monitored continuously. In Fig. 9 the specular intensity is plotted versus the estimated surface temperature. There is little attenuation of the specular beam in going from room temperature to 900 °C, indicating a very high Debye temperature, but there is an abrupt irreversible drop above this temperature. No specular intensity could be detected after cooling from 990 °C.

Then hydrogen was admitted at $p \simeq 10^{-5}$ Torr for >10 min as described in Ref. 14, but no improvement in the signal was detected. In Ref. 14 certain electron energy-loss spectrum features in the band gap, tentatively assigned to empty surface states, appeared only for the reconstructed surfaces, and upon introduction of hydrogen these features disappeared. If H were responsible for the diffraction pattern of the untreated surface this exposure might have restored the (1×1) periodicity. Subsequently, a LEED pattern was taken and a faint $(2\times2)/(2\times1)$ pattern was observed, confirming the persistence of the reconstruction. It is deduced from the very low specular intensity that the topmost layer is very disordered. Previous experience (see Sec. II B) indicates that this disorder cannot be annealed out. Hydrogen was also introduced into the apparatus as described above with our good unreconstructed surface. No change in the ^{4}He reflection intensity was detected during or after this treatment.

VI. CONCLUSIONS

The scattering of ^{4}He atoms from the (111) diamond surface has been investigated. A great deal of effort was put into preparing the surface. The small reflected intensities obtained suggest that the surface is partially disordered. Nevertheless, the results presented are very reproducible, and meaningful comparisons with the He-graphite case can be made. The occurrence of a $(2\times2)/(2\times1)$ reconstruction was also studied. A better surface would have been very useful to obtain structural information on the reconstructed surface.

ACKNOWLEDGMENTS

The authors thank the National Science Foundation for their support of this work under Grants Nos. DMR 7722961 and 8023225, and the DeBeers Industrial Diamond Division for the loan of the sample. Mr. Wai Leung is thanked for much technical assistance and Professor Milton W. Cole and Dr. Robert Laughlin are thanked for numerous helpful discussions.

---

*Present address: Division of Chemistry and Chemical Engineering, California Institute of Technology, Pasadena, CA 91125.

[1]M. J. Cardillo, Annu. Rev. Phys. Chem. 32, 331 (1981).

[2]T. Engel and K. H. Rieder, *Structural Studies of Surfaces with Atomic and Molecular Beam Diffraction,* Vol. 91 of *Springer Tracts in Modern Physics* (Springer, Berlin, 1981).

[3]M. J. Cardillo, G. E. Becker, S. J. Sibener, and D. R. Miller, Surf. Sci. 107, 469 (1981).

[4]M. J. Cardillo, G. E. Becker, and J. A. Serri, in Proceedings of the 42nd Annual Conference on Physical Electronics, Atlanta, 1982 (in press).

[5]G. Derry, D. Wesner, W. E. Carlos, and D. R. Frankl, Surf. Sci. 87, 629 (1979); G. Derry, D. Wesner, G. Vidali, T. Thwaites, and D. R. Frankl, *ibid.* 94, 221 (1980).

[6]G. Boato, P. Cantini, and R. Tatarek, Phys. Rev. Lett. 40, 887 (1978); G. Boato, P. Cantini, R. Tatarek, and G. P. Felcher, Surf. Sci. 80, 518 (1979).

[7]G. Brusdeylins, R. B. Doak, and J. P. Toennies, Phys. Rev. Lett. 44, 1417 (1980).

[8]W. E. Carlos and M. W. Cole, Phys. Rev. B 21, 3713 (1980); Surf. Sci. 91, 339 (1980).

[9]R. L. Elgin, J. M. Greif, and D. L. Goodstein, Phys. Rev. Lett. 41, 1723 (1978).

[10]H. W. Weinberg and R. P. Merrill, in *Adsorption-Desorption Phenomena,* edited by F. Ricca (Academic, New York, 1972).

[11]J. B. Marsh and H. E. Farnsworth, Surf. Sci. 1, 3 (1964); J. J. Lander and J. Morrison, *ibid.* 4, 241 (1966).

[12]P. G. Lurie and J. M. Wilson, Surf. Sci. 65, 453 (1977).

[13]F. J. Himpsel, J. A. Knapp, J. A. van Vechten, and D. E. Eastman, Phys. Rev. B 20, 624 (1979); B. B. Pate, W. E. Spicer, T. Ohta, and I. Lindau, J. Vac. Sci. Technol. 17, 1087 (1980).

[14]S. V. Pepper, Appl. Phys. Lett. 38, 344 (1981); J. Vac. Sci. Technol. 20, 213 (1982).

[15]J. Ihm, S. G. Louie, and M. L. Cohen, Phys. Rev. B 17, 769 (1971).

[16]L. F. Wagner and W. E. Spicer, Phys. Rev. Lett. 28, 1381 (1972); D. E. Eastman and W. D. Grobman, *ibid.* 28, 1378 (1972).

[17]M. L. Cohen, Phys. Rev. B 22, 1095 (1980).

[18]F. J. Himpsel, D. E. Eastman, and F. J. Van der Veer, J. Vac. Sci. Technol. 17, 1085 (1980); B. B. Pate, P. M. Stefan, C. Binns, P. J. Jupiter, M. L. Shek, I. Lindau, and W. E. Spicer, *ibid.* 19, 349 (1981).

[19]G. Derry, D. Wesner, S. V. Krishnaswamy, and D. R. Frankl, Surf. Sci. 74, 245 (1978).

[20]The diamond sample was kindly provided by DeBeers Industrial Diamond Ltd., Johannesburg, South Africa.

[21]G. Vidali, Ph.D. thesis, The Pennsylvania State University, 1982 (unpublished).

[22]G. Braunstein, Radiat. Eff. 48, 139 (1980); F. A. Raal (DeBeers Ltd.) (private communication); also Refs. 11 and 12.

[23]See for example H. Hoinkes, Rev. Mod. Phys. 52, 933 (1980).

[24]E. M. Lifshitz, Zh. Eksp. Teor. Fiz. 29, 94 (1955) [Sov. Phys.—JETP 2, 73 (1956)]; for $z > 100$ Å, retardation modifies this result.

[25]G. Vidali and M. W. Cole, Surf. Sci. 107, L374 (1981).

[26]G. Vidali, M. W. Cole, and C. Schwartz, Surf. Sci. 87, L273 (1979).

[27]U. Garibaldi, A. C. Levi, R. Spadacini, and G. E. Tommei, Surf. Sci. 48, 649 (1975).

[28]The uncertainty given for ξ_{10} corresponds to a 50% variation in the value of $\chi=\sum(P_e-P_t)^2/N$ from its minimum (for $\xi_{10}=0.021$ Å), where P_e and P_t are the experimental and theoretical probabilities, respectively.

[29]G. Boato, P. Cantini, and L. Mattera, Surf. Sci. 55, 141 (1976).

[30]G. Boato, P. Cantini, and R. Tatarek, J. Phys. F 6, L237 (1976); in *Proceedings of the Third International Conference on Solid Surfaces,* edited by R. Dobrozemski *et al.* (IEAE, Vienna, 1977), p. 1377.

[31]R. B. Laughlin, private communication.

[32]R. B. Laughlin, Phys. Rev. B 25, 2222 (1982).